



Missouri University of Science and Technology
Scholars' Mine

International Conferences on Recent Advances
in Geotechnical Earthquake Engineering and
Soil Dynamics

2010 - Fifth International Conference on Recent
Advances in Geotechnical Earthquake
Engineering and Soil Dynamics

27 May 2010, 4:30 pm - 6:20 pm

Comparison of Liquefaction Triggering Analysis Approaches for an Embankment Dam and Foundation

David C. Serafini

U.S. Army Corps of Engineers, Sacramento, CA

Vlad Perlea

U.S. Army Corps of Engineers, Sacramento, CA

Follow this and additional works at: <https://scholarsmine.mst.edu/icrageesd>

 Part of the [Geotechnical Engineering Commons](#)

Recommended Citation

Serafini, David C. and Perlea, Vlad, "Comparison of Liquefaction Triggering Analysis Approaches for an Embankment Dam and Foundation" (2010). *International Conferences on Recent Advances in Geotechnical Earthquake Engineering and Soil Dynamics*. 10.

<https://scholarsmine.mst.edu/icrageesd/05icrageesd/session04b/10>

This Article - Conference proceedings is brought to you for free and open access by Scholars' Mine. It has been accepted for inclusion in International Conferences on Recent Advances in Geotechnical Earthquake Engineering and Soil Dynamics by an authorized administrator of Scholars' Mine. This work is protected by U. S. Copyright Law. Unauthorized use including reproduction for redistribution requires the permission of the copyright holder. For more information, please contact scholarsmine@mst.edu.



Fifth International Conference on

Recent Advances in Geotechnical Earthquake Engineering and Soil Dynamics and Symposium in Honor of Professor I.M. Idriss

May 24-29, 2010 • San Diego, California

COMPARISON OF LIQUEFACTION TRIGGERING ANALYSIS APPROACHES FOR AN EMBANKMENT DAM AND FOUNDATION

David C. Serafini, M.S., P.E.

US Army Corps of Engineers, Sacramento District
1325 J Street, Sacramento, CA 95814

Vlad Perlea, Ph.D., P.E.

US Army Corps of Engineers, Sacramento District
1325 J Street, Sacramento, CA 95814

ABSTRACT

Success Dam is located on the Tule River, near the city of Porterville, California. The dam is a rolled earth-fill embankment approximately 145 feet high and 3,400 feet long. The embankment is comprised of a central impervious core protected by upstream and downstream outer pervious zones. A majority of the dam is founded on potentially liquefiable Holocene alluvium. Several analytical techniques of varying complexity have been used to determine the liquefaction potential of the foundation Holocene alluvium and the pervious embankment shells. The following analytical techniques were used on the Success Dam Remediation Project: (1) cyclic stress ratio (CSR) evaluation using peak shear stresses obtained from QUAD4M equivalent linear seismic response type analyses, (2) evaluation of QUAD4M element shear stress time histories using a cycle counting approach to approximate the potential excess pore water pressure ratios, and (3) more advanced non-linear dynamic FLAC analyses using UBCSAND to evaluate excess pore water pressure ratios for potentially liquefiable materials.

This paper discusses the approaches taken to evaluate the liquefaction potential for the seismic assessment and remediation design of the existing dam. This paper also summarizes the advantages and limitations of each of each analytical approach used to evaluate liquefaction potential of the dam and foundation materials.

INTRODUCTION

Success Dam is located on the Tule River approximately five miles upstream of Porterville, California. Construction of the dam began in 1958 and was completed in 1961. Investigations and studies under the Corps of Engineers Dam Safety Assurance Program (DSAP) demonstrated that remediation is required to prevent dam failure and reservoir release due to potential large deformation of the dam resulting from strength loss of the foundation and embankment materials from a large earthquake.

The Corps of Engineers is currently designing the seismic remediation of Success Dam. Explorations conducted for remediation design revealed detrimental foundation characteristics that were more widespread and more complex than was previously known. In addition, more recent seismic stability evaluations also found the dam deficient according to current requirements and methods of evaluation. As a consequence, remediation of the dam is required. The reservoir is currently operated under restriction, with the maximum pool 22.5 feet below the normal gross pool

(spillway crest elevation), which reduces the available reservoir storage by about 50%. The design team developed and calibrated the methodology of seismic response and deformation analysis to be used in design of the remediation. This paper discusses the approaches taken to evaluate the liquefaction potential for the seismic assessment and remediation design of the existing dam, and also summarizes the advantages and limitations of each of each analytical approach.

BACKGROUND

The characterization of the Success Dam site has been an ongoing and challenging process. This section provides a summary of the existing embankment design and materials, an overview of the foundation conditions, a summary of the pertinent field investigations and material properties, and an overview of the site seismicity.

Existing Embankment Design and Materials

Success Dam is about 145 feet high, providing 39 feet of freeboard above the normally full (gross) pool, and 4.7 feet of freeboard above the maximum spillway design flood elevation. The embankment is comprised of a central impervious core supported by upstream and downstream transition and outer pervious zones. The upstream slope of the dam transitions from 1:3.75 at the toe, 1:3 midway up the slope, and 1:2.5 at the crest. The downstream slope is 1:3 at the toe and steepens to 1:2.5 at the crest. A typical cross section of the embankment is shown in Figure 1.

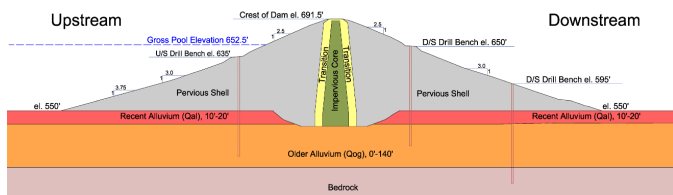


Figure 1. Typical Embankment Cross Section and Exploration Bench Locations.

The impervious core is predominantly sandy clay and clayey sand. The core material was placed in 12-inch loose lifts and compacted by 4 passes of a 50-ton pneumatic-tired roller. The transition zones are gravelly sands and the pervious zones were constructed with sand and rock sizes smaller than 12 inches obtained from recent alluvium deposits and from spillway excavation. The pervious shell materials are generally classified as gravelly sand with an 18 inch maximum particle size and no more than 12% passing the No. 200 sieve. The large size particles made drilling, sampling, and characterization of the embankment shells very difficult. A majority of the pervious embankment shell material was constructed from the recent alluvium foundation, and therefore, has a similar composition. Construction records indicate the pervious zones were placed in 24-inch loose lifts with a tracked dozer and compacted by 4 passes of a 50-ton pneumatic-tired roller. Portions of the pervious shells were found in a relatively loose state and are potentially liquefiable.

Foundation Conditions

Foundation soils include alluvial, residual, and slopewash soils. Alluvial soils include: recent alluvium, older alluvium, terrace deposits, and fan deposits. Residual soils were formed by weathering of the bedrock complex and the alluvial terrace deposits, while slopewash material is present where movement of the residual soils by gravity has occurred. A cross-valley profile of the foundation soil, approximately along the dam axis, is presented in Figure 2.

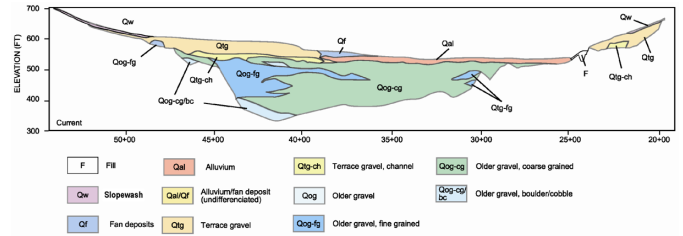


Figure 2. Geologic Cross-Valley Profile.

Loose Holocene recent alluvium, noted in Figure 2 with Qal, underlies the upstream and downstream shells of the dam for approximately 50% of the dam's footprint. The recent alluvium deposit ranges in thickness approximately between 10 and 20 feet and consists of materials that are unconsolidated, frequently loose, and totally uncemented. The recent alluvium is mainly an assortment of interbedded sands and sandy gravels with generally less than 10% non-plastic fines and occasional cobbles and boulders. The sand is medium to fine-grained. The gravel is fine to coarse and the cobbles and boulders range from 3 inches to 3 feet, which made characterization through penetration tests difficult.

Field Investigations and Material Properties

Gravels and cobbles in both the foundation alluvium and shell material was a major challenge in the selection of parameters for deformation analysis, in particular those related to the liquefaction potential and the residual strength. Penetration testing of the recent alluvium to estimate its liquefaction potential was very challenging. Both the Standard Penetration Test (SPT) and the Becker Hammer Penetration Test (BPT) were used. A site specific correlation between SPT and BPT data was established. However, the gravel, cobble and boulder content of the material made it difficult to test and sample using the conventional. Most penetration testing was subjected to considerable interpretation given the quantity of large particles and the drilling difficulty. Therefore, cross-hole shear wave velocity (V_s) measurements were taken extensively throughout the site as a companion method.

The liquefaction potential was estimated using $N_{1,60}$ data from SPT's and BPT's, and stress corrected V_s data (V_{s1}) from cross-hole tests. For developing a correlation between $N_{1,60}$ and V_{s1} , the liquefaction assessment criterion by Andrus and Stokoe (2000) was used. A comprehensive analysis of data in literature indicated that the criterion by Andrus and Stokoe is more conservative than the $N_{1,60}$ -based criterion (Youd et al., 2001), as shown in some detail by Serafini et al., 2008.

Penetration test results and shear wave velocities measurements obtained in the recent alluvium and at various locations in the pervious embankment shell have indicated the materials to be potentially liquefiable ($N_{1,60} < 30$ blows/ft). In the recent alluvium the typical $N_{1,60}$ design values were

assigned to be between 10 and 21 blows/ft. A design $N_{1,60}$ value of 18 blows/ft was assigned to the upstream pervious embankment shell material at one of the representative cross sections. Table 1 presents the strength parameters of various materials within the embankment and foundation as they were input in the deformation analyses of one of the representative cross sections. Conservative $N_{1,60}$ values (approximately 33rd-percentile) were selected for design because of the high variability of the results and the relatively low confidence in penetration tests.

Table 1. Strength Parameters of Materials

Material (Material ID, see Figure 5)	V_{s1} (fps)	$N_{1,60}$ (bpf)	Shear Strength Parameters			
			Effective		Total**	
			ϕ' (°)	c' (psf)	ϕ (°)	c (psf)
Upstream shell:						
-upper (ES1_1)	650	26	37	0	0	3800
-lower (ES1_2)	550	18	37	0	0	870
Downstream shell (ES1_3)	700	26	37	0	0	3800
Impervious core (EC_1)	550	-	17	540	11	740
Recent alluvium:						
-below u/s slope (RA_1)	450	10	36	0	0	250
-below d/s slope (RA_2)	690	21	36	0	0	1450
-free field (RA_3)	640	10	36	0	0	250
Older alluvium						
-below u/s slope (OA_1)	1000	-	36	0	30	2000
-below d/s slope (OA_2)	1250	-	36	0	30	2000
Saprolite (weathered rock)	450	7*	24	400	24	400
Bedrock:						
-upper (Rock_1)	2800	-	assumed elastic material			
-lower (Rock_2)	4000	-	assumed elastic material			

Notes: * The Saprolite was not considered liquefiable, so $N_{1,60}$ was not used in the analyses.

** For the materials assumed liquefiable (shell materials and recent alluvium) the post-liquefaction residual strength is listed.

Site Seismicity

The existing dam and potential remediation variants have been evaluated for two levels of earthquake loading: the Operational Basis Earthquake (OBE) and the Maximum Credible Earthquake (MCE). The OBE design criterion is primarily used to address economic concerns. In simple terms, the dam should survive the OBE without significant damage or the need for expensive repairs. The MCE level of loading is for the evaluation of life-safety concerns. Although significant damage may be anticipated, the dam must survive the MCE without producing conditions that lead to an uncontrolled release of the reservoir.

Seismic loading parameters were developed by URS Corporation (URS) based on the target parameters summarized in Table 2, in terms of moment magnitude (M_w), distance to site (D), and peak horizontal ground acceleration (PGA). The goal was to select seismic time histories with parameters within the range specified under parentheses in Table 2. The primary local seismic sources are presented in Figure 3.

Table 2. Seismic Design Criteria

Design Earthquake	M_w	D (km)	PGA (g)
OBE (probabilistic: 144-year average return period)	8.0 (7.3-8.0)	120 (60-240)	0.10 (0.05-0.2)
MCE (deterministic : 84th percentile)	6.8 (6.5-7.0)	21 (10-42)	0.28 (0.14-0.56)

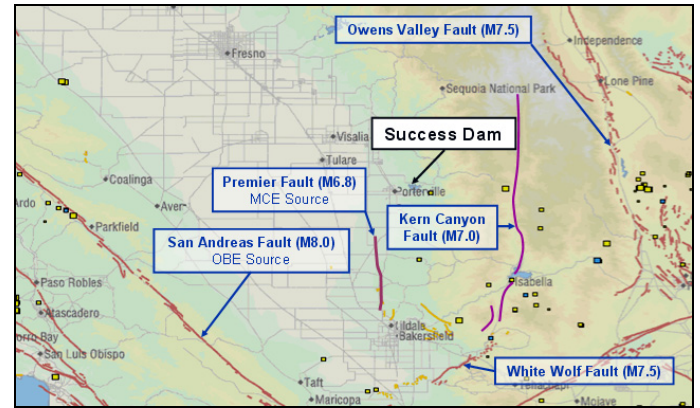


Figure 3. Primary Seismic Sources in Vicinity of Success Dam.

Ten available strong earthquake records, two horizontal components each, were selected by URS to represent OBE and MCE loading at the dam site. Each record was scaled for best fit with the target spectrum in the range of dominant response periods (0.1 s to 1.0 s) and was subsequently deconvoluted to account for the bedrock layers included in the FLAC model. These records are listed in Table 3 and 4, for OBE and MCE respectively.

Table 3. OBE Time Histories

ID	Earthquake	M_w	Station	Duration (sec)	Component	Scaling Factor
#1	Chi-Chi, Taiwan				N	1.516
#2	1999/09/20	7.6	ENA	82	E	1.403
#4	Kocaeli, Turkey				000	2.358
#5	1999/08/17	7.4	Mecidiyekoy	41	090	2.052
#7	Denali, Alaska				066	1.468
#8	2002/11/03	7.9	TAP Pump Station #11	145	336	1.377
#10	Denali, Alaska				013	1.803
#11	2002/11/03	7.9	TAP Pump Station #9	145	103	1.546
#13	El Salvador				180	1.117
#14	2001/01/13	7.6	Acajutla Cepa	50	270	1.464

Table 4. MCE Time Histories

ID	Earthquake	M _w	Station	Duration (seconds)	Component	Scaling Factor
#1	Loma Prieta		Santa Teresa hill		225	1.081
#2	1989/10/18	6.9		50	315	1.095
#4	Northridge		San Gabriel		180	2.112
#5	1994/01/17	6.7	E Grand Ave	34.6	270	1.702
#7	San Fernando		Castaic – Old Ridge R.		021	1.254
#8	1971/02/09	6.6		30	291	1.028
#10	Loma Prieta		Gilroy Array		000	1.773
#11	1989/10/18	6.9	# 6	39.5	090	1.441
#13	Imperial Valley		Cerro Prieto Station		147	1.418
#14	1979/10/12	6.5		56.6	237	1.080

Notes: M_w = moment magnitude; Scaling factor before deconvolution.

SEISMIC ANALYSIS PROCEDURES

Several analytical techniques of varying complexity were used to determine the liquefaction potential of the foundation Holocene alluvium and the pervious embankment shells, and the resulting deformation of the embankment. The following analytical techniques were used for the evaluation: (1) cyclic stress ratio (CSR) evaluation using peak shear stresses obtained from QUAD4M equivalent linear seismic response type analyses, (2) evaluation of QUAD4M element shear stress time histories using a cycle counting approach to approximate the potential excess pore water pressure ratios, and (3) more advanced non-linear dynamic FLAC analyses using UBCSAND to evaluate excess pore water pressure ratios for potentially liquefiable materials. The more advanced non-linear dynamic FLAC analyses are discussed first since the FLAC model was also used to generate the initial QUAD4M mesh.

FLAC Analyses with UBCSAND

Methodology. The computer program FLAC (Fast Lagrangian Analysis of Continua), commercially available from Itasca Consulting Group, Inc. (2008), was used in the analyses. FLAC is a two-dimensional finite difference program that solves dynamic problems in the time domain. The program follows an explicit formulation, meaning that it solves the dynamic equations of motion at each nodal mass at every timestep. This scheme is useful for solving highly non-linear problems or those involving large changes in geometry. The primary drawback consists in the small timesteps required for numerical stability of most solutions.

FLAC provides several constitutive models that are useful for many situations. FLAC also allows the users to specify their own constitutive models when additional refinements or features are needed. The user-defined model UBCSAND was used for the liquefiable zones in Success Dam to better model the pre- and post-liquefaction behavior of these zones. Figure 4 shows the use of various constitutive models to model the

behavior of various materials within Success Dam and its foundation.

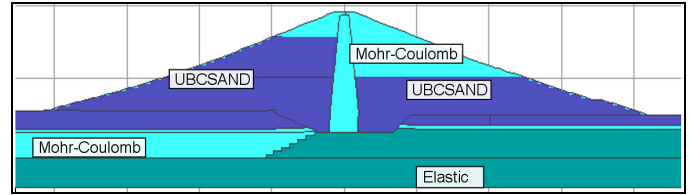


Figure 4. Constitutive models used for dynamic analysis of Success Dam at Station 28+50.

The UBCSAND model was originally developed at the University of British Columbia, Canada (Byrne et al., 2004). To properly model the dynamic behavior of Success Dam and, actually, of any embankment founded on shallow liquefiable soil, the original model was modified by Dr. Michael Beaty. The primary revisions made to the original UBCSAND model improved its behavior in situations with moderate cyclic loading and where there was a significant static bias (existence of relatively large static shear stresses on horizontal planes); conditions encountered under the lower portions of the embankment shells. These revisions were prompted by a careful review of the initial Success Dam analysis results. To improve the prediction of liquefaction under these loading conditions, the ability to generate plastic shear strains during a reload cycle was included into UBCSAND (Rutherford et al., 2008).

Pre-Earthquake Static Equilibrium. The construction of the dam was simulated solving for equilibrium of the foundation without any embankment and then for the addition of each layer of embankment elements. Reservoir loading was added and seepage analysis was performed with FLAC until a steady state condition for the gross pool (crest of spillway elevation) was reached. Note that the steady state condition was used as the initial stress state to develop the QUAD4M input files. Once the initial stress state had been achieved, the model was converted to address dynamic conditions: (a) Adjusting properties of Mohr-Coulomb and elastic zones to address the anticipated dynamic response of the elements; (b) Assigning the UBCSAND model to zones considered susceptible to liquefy (based on possible saturation and $N_{1,60} < 30$, see Table 1 and Figure 4); (c) Assigning appropriate levels of viscous (Rayleigh) damping to various zones; (d) Converting the boundary conditions of the model so that free-field boundaries were used on the left and right boundaries of the model and a compliant (non-reflecting) base is used at the bottom of the model; (e) Setting up FLAC to use large strain formulation, under which the grid geometry is periodically updated to reflect the displacement predictions, allowing changes in geometry to be considered in the stability of the model and in the potential for displacements to develop. Figure 5 shows the cross section at Station 28+50 and the finite difference mesh.

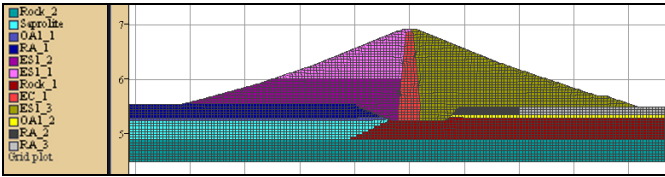


Figure 5. Cross Section and Finite Difference Mesh.

Earthquake Simulation. The time histories for the OBE and MCE earthquakes from Tables 3 and 4 were applied assuming the positive recorded direction was aligned with the positive X-axis of the model and also in a reversed orientation (or “negative”). The change of polarity had a significant effect on the induced displacement in most cases. There were, therefore, 20 computer runs for 20 time histories for both OBE and MCE design level events.

The compliant boundary required the input acceleration history to be converted into an equivalent shear stress history. Because the earthquake motion, in terms of shear stress, was applied to the base of the mesh (within rock), the time history had to be deconvoluted, i.e., modified in such a way that, when applied to the base of the mesh, the desired design time history would be obtained at the top of weathered rock near surface.

Post-Earthquake Analysis. After running for an additional five seconds, to permit decay of motions after the end of the earthquake, the liquefied zones were converted to a Mohr-Coulomb model with residual strengths. For Success Dam, the determination of a liquefied zone was based on elements that had achieved a peak excess pore pressure ratio greater than 0.7 at any time during shaking. The excess pore pressure ratio was defined through the relationship $r_u = 1 - \sigma'_v / \sigma'_{v0}$, where σ'_v is the vertical effective stress at the time that r_u is defined and σ'_{v0} is the initial vertical effective stress (just before the earthquake occurrence). The residual strength used in the FLAC model was based on the Seed and Harder (1990) correlation with $N_{1,60}$, using the relationship proposed by Idriss and Boulanger (2007).

Liquefaction Evaluation Using QUAD4M Analyses

Methodology. The results of the FLAC seismic deformation analysis were compared with the results of more simplified analyses using QUAD4M coupled with the simplified liquefaction procedure. The QUAD4M mesh was created from the FLAC model using a FISH routine, which converted the FLAC (i,j) grid to equivalent QUAD4M (x,y) elements and nodes. The FISH routine created a QUAD4M input file with the same geometry, stiffness (Gmax), and unit weight as the FLAC model. All QUAD4M materials except for bedrock were assigned variable Gmax values based on the FLAC analysis pre-earthquake (static) stress state. The equivalent QUAD4M finite element mesh for the cross section at Station

28+50 is shown in Figure 6 and a summary of the assigned zones is included in Table 5.

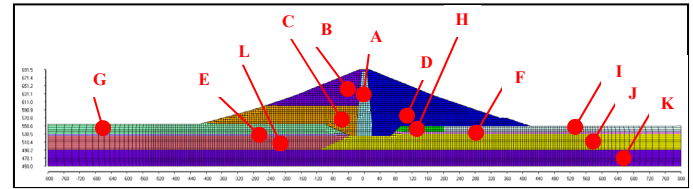


Figure 6: Station 28+50, Existing Dam Mesh and Primary Zones (12 Zones).

Table 5. Summary of the QUAD4M Zones and G/Gmax and damping Curve Set Assignment.

Zone	Zone Description	QUAD4M Material Number	Gmax (ksf)	Gmax and Damping Curve Set
A	EC_1	1	Variable	I
B	ES1_1	2	Variable	III
		3		IV
C	ES1_2	4	Variable	III
		5		IV
		6		V
D	ES1_3	7	Variable	III
		8		IV
		9		V
E	OA1_1	10	Variable	III
		11		IV
		12		V
F	OA1_2	13	Variable	III
		14		IV
		15		V
G	RA_1	16	Variable	III
		17		IV
		18		V
H	RA_2	19	Variable	IV
I	RA_3	20	Variable	III
		21		IV
		22		V
J	Rock_1	23	33,000	II
K	Rock_2	24	67,000	II
L	Saprolite	25	Variable	III
		26		IV
		27		V

A FISH routine was also used to assign variable G/Gmax and damping curve sets for each of the materials/zones. A summary of the variable G/Gmax and damping curve set

assignment is shown in Figure 7 and also included in Table 5. Five different curve sets were used in the QUAD4M analyses for the analysis of the existing dam. The G/Gmax and damping curve sets are described below and are shown graphically in Figures 7 and 8, respectively.

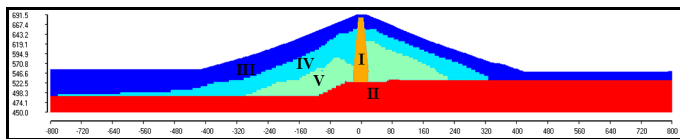


Figure 7: Variable G/Gmax and Damping Curve Sets Assigned to the Mesh at Station 28+50.

Impervious core materials were assigned to Curve Set I. Bedrock materials were assigned to Curve Set II. The selection of the shear modulus reduction and damping curves for coarse-grained materials were based on the FLAC pre-earthquake effective stress (σ_{vo}) of the layer.

Curve Set I: Impervious Core
 G/Gmax: CLAY (PI=20-40 Sun et al. 1988)
 Damping Curve: CLAY Average (Seed & Idriss 1970)

Curve Set II: Bedrock
 G/Gmax: ROCK (Schnabel 1973)
 Damping Curve: ROCK (Schnabel 1973)

Curve Set III: Bedrock Pervious Shell Material and Alluvial Foundation Material (for $\sigma_{vo}' < 4000$ psf)
 G/Gmax: SAND Lower Bound (Seed & Idriss 1970)
 Damping Curve: SAND Upper Bound (Seed & Idriss 1970)

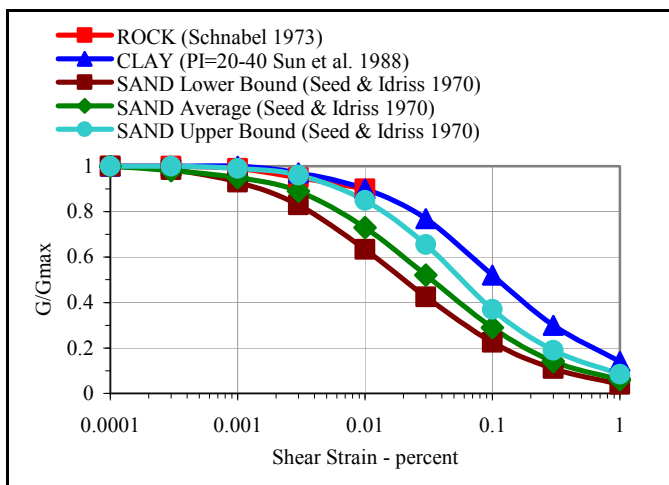


Figure 7: Summary Plot of the Selected G/Gmax Curves.

Curve Set IV: Bedrock Pervious Shell Material and Alluvial Foundation Material (for $4000 \leq \sigma_{vo}' < 8000$ psf)
 G/Gmax: SAND Average (Seed & Idriss 1970)

Damping Curve: SAND Average (Seed & Idriss 1970)

Curve Set V: Bedrock Pervious Shell Material and Alluvial Foundation Material (for $\sigma_{vo}' \geq 8000$ psf)
 G/Gmax: SAND Upper Bound (Seed & Idriss 1970)
 Damping Curve: SAND Lower Bound (Seed & Idriss 1970)

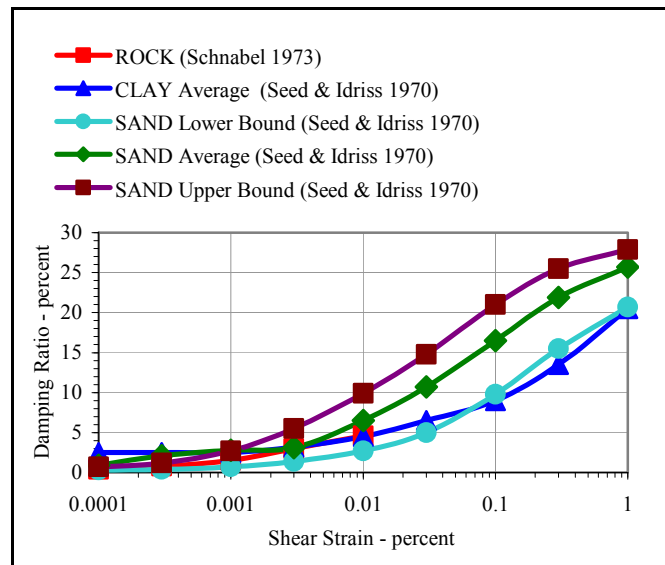


Figure 8: Summary Plot of the Selected Damping Curves.

QUAD4M was used as a complementary method to estimate the cyclic induced shear stresses in materials that have the potential for liquefaction. For these materials the peak cyclic shear stresses were obtained from the QUAD4M output and used with the simplified liquefaction procedure to estimate a factor of safety against liquefaction ($F.S._{LIQ}$). The simplified $F.S._{LIQ}$ was compared to a slightly more rigorous but still simplified procedure involving the counting of shear stress cycles in selected QUAD4M elements to estimate excess pore water pressure ratios. The two procedures resulted in a comparison between the $F.S._{LIQ}$ and the potential excess pore water pressure ratio (r_u).

Simplified $F.S._{LIQ}$ Calculation. The simplified $F.S._{LIQ}$ was calculated using a simple FISH code in FLAC. The $F.S._{LIQ}$ computations were performed at the same stress state that dynamic loading is applied in the UBCSAND constitutive model. The cyclic stress ratio (CSR) was estimated using the peak shear stresses from the QUAD4M output. The cyclic resistance ratio (CRR) was approximated using the $N_{1,60}$ field performance relationship by Boulanger and Idriss (2004a). The magnitude scaling factor (MSF) and the overburden stress correction (K_σ) were also estimated using the relationships by Boulanger (2003b). The static shear stress ratio correction factor (K_α) was approximated using the relationship by Boulanger (2003a). The $F.S._{LIQ}$ calculated using the simplified method was used to estimate r_u by using Figure 15,

and the average to upper bound gravels curve by Marcuson et al., 1990. The selection of a $F.S._{LIQ} - r_u$ relationship was also based on using cycle counting to estimation of r_u , and is covered in the results section of the paper.

Cycle Counting and estimation of r_u . The QUAD4M shear stress time history files for selected elements were used in a slightly more rigorous method of the simplified procedure to estimate the potential excess pore water pressure for the element. The QUAD4M elements selected for the cycle counting procedure are shown in Figure 9. The computations were performed using an Excel spreadsheet to estimate the number of equivalent shear stress half cycles (Neq) for a selected element at an average stress level of $0.65\tau_{max} / \sigma_{v0}$ and to estimate r_u based on the number of cycles required for liquefaction (Nliq). Neq was determined using the average of two cycle counting methods described by Idriss and Boulanger (2004b), and Green and Terri (2005).

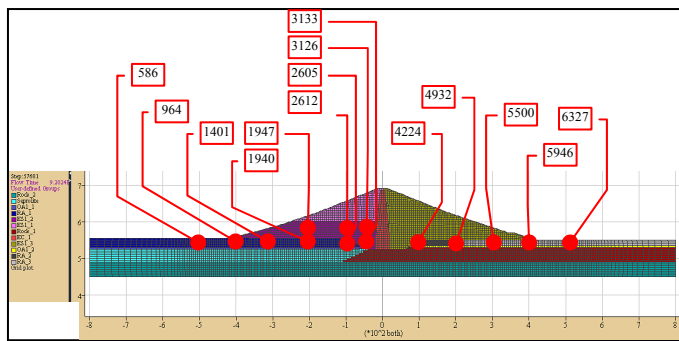


Figure 9: QUAD4M Elements Selected for the Cycle Counting Procedure.

The number of cycles required for liquefaction (Nliq) for a given element was calculated using a method based on the simplified procedure. The method coupled the empirical $N_{1,60}$ -CRR field performance relationship and magnitude scaling factor (MSF) relationship (both from Idriss and Boulanger, 2004a) to develop a relationship for CSR-Nliq (for $F.S._{LIQ} = 1.0$, where $CRR=CSR$). Therefore, CRR or CSR is adjusted using the MSF for the number of cycles for liquefaction (Nliq). An approximate relationship was developed for the number of cycles for liquefaction as shown in Equation (1) below.

$$Nliq = 0.013 \exp\left[0.1625N_{1,60}\right] \left(\frac{CSR}{K_\sigma K_\alpha}\right)^{-2.4976} \quad (1)$$

It should be noted that several different cycle counting procedures were evaluated and compared. One procedure accounted for the initial static shear stress of each element and only counted shear stress cycles that increased the shear stress (above static) or that experienced an unloading of the shear stress near or past the point of a stress reversal. A closer comparison of predicted r_u between the simplified procedure

and the UBCSAND model was obtained by applying K_α in the cycle counting procedure. The application of K_α helped incorporate in the analysis the materials relative density ($N_{1,60}$ value) and the effects of the initial static shear stress.

SEISMIC ANALYSIS RESULTS

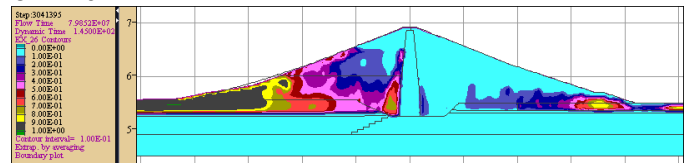
The dam behavior was evaluated under both OBE and MCE loading for a number of representative time histories as shown in Tables 3 and 4. This paper focuses on the comparison of liquefaction triggering for MCE records 1, 4, 8, 11, and 14, and for OBE records 2, 4, 8, 10 and 14, all applied with their critical orientation. Detailed comparisons between three different methods are shown specifically for OBE #8 and MCE #14, since they were the most damaging records from each of the time history sets. The MCE set of records included a wide range in duration and number of significant cycles. After scaling to the target spectrum and deconvolution, the peak ground acceleration for the MCE events varied between 0.16g and 0.26g.

FLAC Analyses with UBCSAND

The critical time histories that produced the largest extent of liquefaction were found to be the ones with the longest duration, both in OBE and MCE cases. Since the probabilistic OBE motion is expected to be generated by a magnitude 8 earthquake, long shaking duration is highly probable. Therefore, the results computed with these long records should be considered representative.

It is evident from Figure 10 that almost the entire recent alluvium in the foundation and the lower portion of the upstream shell liquefied ($r_u > 0.7$) following the MCE event, but the extent of liquefaction was much smaller under OBE loading, especially downstream of the core. The extent of liquefaction reflected directly in the amount of displacements, as illustrated in Figure 10.

OBE #8



MCE #14

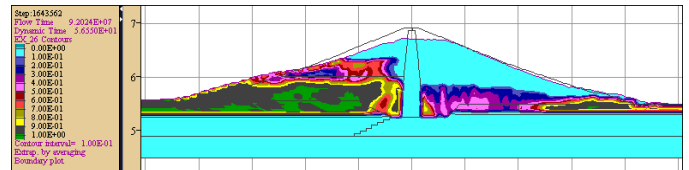


Figure 10. Excess Pore Pressure Ratio at the End of Shaking for OBE #8 and MCE #14.

The most critical time history for liquefaction triggering and embankment deformation was MCE #14. Although this record had the lowest peak ground acceleration (0.16g) it had the longest duration (56.6 s) of all considered MCE time histories. It is possible that MCE #14 may not be representative of a magnitude 6.8 seismic event, as desired, because of its unusually large number of significant cycles.

Liquefaction Evaluation Using QUAD4M Analyses

The liquefaction analyses using QUAD4M and the simplified method were primarily used as a check for the FLAC seismic deformation analyses. Therefore, additional focus was placed on the MCE results where the extent of liquefaction potential was significant. A comparison of r_u for the MCE load cased is shown in Figure 11. Based on the results on Figure 11, each MCE generally estimated about the same extent of liquefaction triggering; however, MCE appeared to produce a slightly larger extend in the recent alluvium layer under the upstream shell.

A comparison of r_u for the OBE load cased is shown in Figure 12. Based on the results on Figure 12, each OBE also generally estimated about the same extent of liquefaction triggering near the upstream and downstream toes of the dam. However, OBE #8 appeared to produce a slightly larger extend of liquefaction triggering in the recent alluvium layer under the upstream shell, and OBE #14 produced a larger extent of liquefaction triggering under the downstream shell.

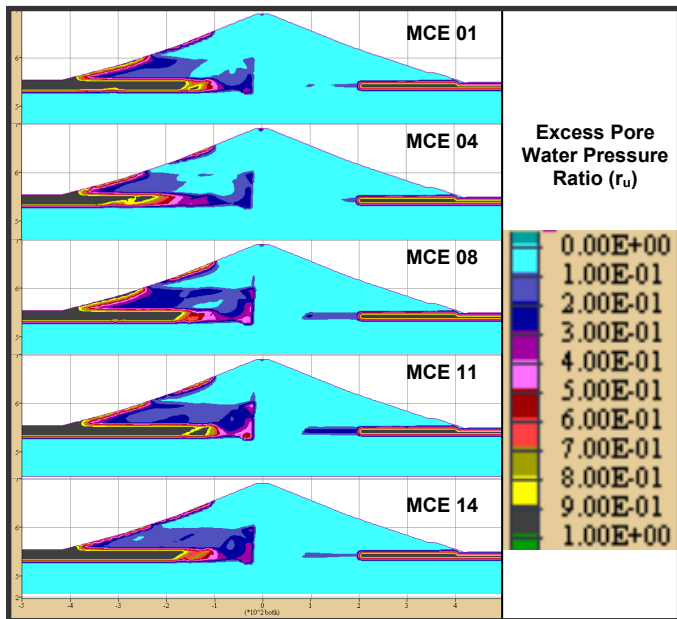


Figure 11. Comparison of r_u for the Existing Dam at Station 28+50 for MCE Loading.

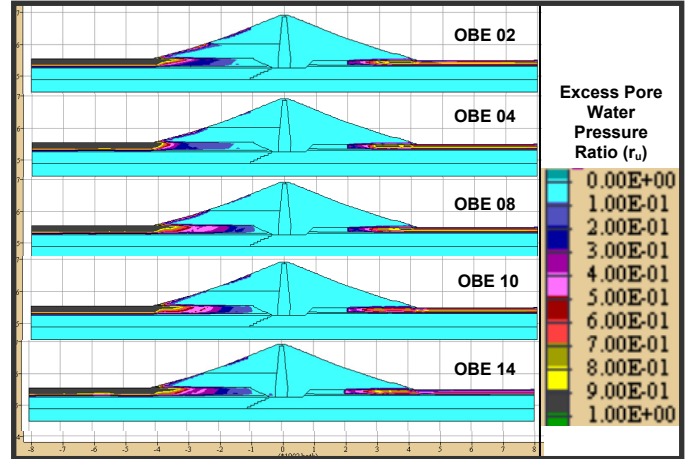


Figure 12. Comparison of r_u for the Existing Dam at Station 28+50 for OBE Loading.

The second method used to estimate the potential excess pore water pressure ratio was by using the shear stress time history files for selected QUAD4M elements, which were shown previously in Figure 9. As described previously, the method involved estimating the number of equivalent shear stress half cycles (N_{eq}) for a selected element at an average stress level of $0.65\tau_{max}/\sigma'_{vo}$ and estimating r_u based on the number of cycles required for liquefaction (N_{liq}). The cycle counting results for the selected MCE time histories are shown in Figures 13 and 14. Figure 13 is a summary of the average stress level ($0.65\tau_{max}/\sigma'_{vo}$) for each of the selected QUAD4M elements under each of the MCE events. Figure 14 is a summary of the number of equivalent shear stress half cycles (N_{eq}) for the selected elements under each of the MCE loadings.

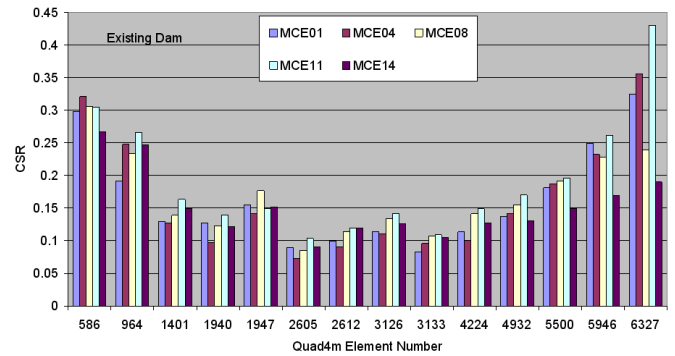


Figure 13. CSR for the Element in the Evaluation

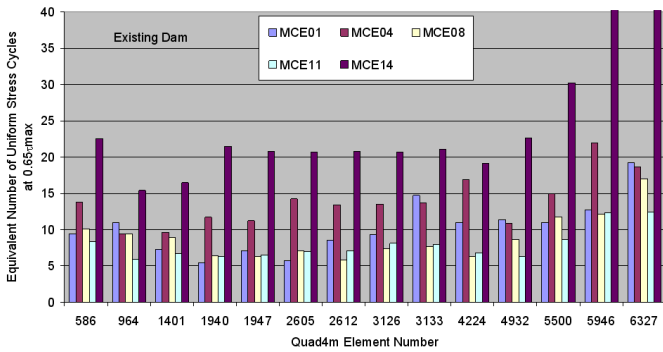


Figure 14. Equivalent Number of Uniform Shear Stress Cycles

In general, Figure 13 indicates that each of the time histories representing the MCE events are generating about the same average level of shear stress in each element. However, Figure 14 shows that the number of equivalent shear stress cycles varied widely and indicated that MCE #14 is somewhat of an outlier which was also shown in the FLAC-UBCSAND analyses for this section at Station 28+50. It should be noted that MCE #14 was not the critical time history with the other evaluated cross section at Station 35+50.

Comparison of r_u to F.S.LIQ

The results of several evaluations using the simplified method to calculate the F.S.LIQ and the cycle counting procedure to estimate r_u were plotted on r_u - F.S.LIQ lab test data graph by Marcuson et al., 1990. As one might expect there was significant scatter in the data, but in general for F.S.LIQ approaching 1.0, plus or minus, r_u was generally in the range of 0.7 to 1.0. The plotted data however did generally indicate higher r_u values for given values of F.S.LIQ on average near the upper bound limits of the Marcuson et al. (1990) curve. Combined plots of r_u versus the F.S.LIQ which include K_{α} in the cycle counting method are shown in Figure 15. Computation of r_u from the cycle counting technique was found to be inefficient and limited since only a few elements could be easily evaluated at a time. Therefore, a relationship was selected for r_u versus F.S.LIQ to simplify the analysis and eliminate the need to count the shear stress cycles for each evaluation. The relationship was used as part of the simplified procedure described above to estimate r_u based on the F.S.LIQ. In general, the relationship may predict slightly more conservative r_u values for $1.2 < F.S.LIQ < 1.8$. The resulting relationship is shown in the Equation (2) below and is also included in Figure 15.

$$r_u = F.S.LIQ^x \quad (\text{for } F.S.LIQ < 3.0) \quad (2)$$

$$x = - \left[F.S.LIQ + \frac{1.9}{F.S.LIQ} + \frac{0.95}{F.S.LIQ^{0.5}} \right]$$

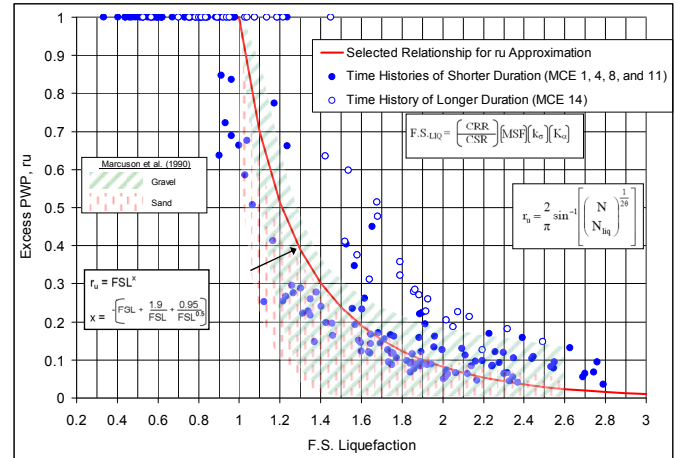


Figure 15. Plot of F.S.LIQ versus r_u ($0.2 < F.S.LIQ < 3$)

The estimated r_u for elements based on the F.S.LIQ results and using Equation (2) for OBE #8 and MCE #14 are presented in Figures 16.

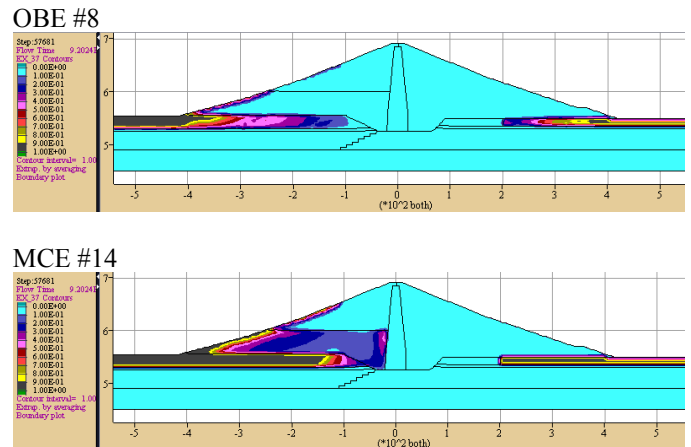


Figure 16. Existing Dam and Estimated r_u for OBE #8 and MCE #14.

Comparison of r_u by the Three Methods

Comparisons made between the three methods demonstrated some of the advantages and limitations in utilizing each approach. In general, the simplified methods and the more advanced FLAC-UBCSAND yielded the same end result under the MCE and OBE loading. The extent of estimated liquefaction in the foundation materials was commonly shown to control the overall stability of the embankment. For the MCE and OBE load cases the same extent of liquefaction was estimated in the foundation materials both upstream and downstream of the existing dam core as demonstrated by comparing Figure 10 and Figure 16.

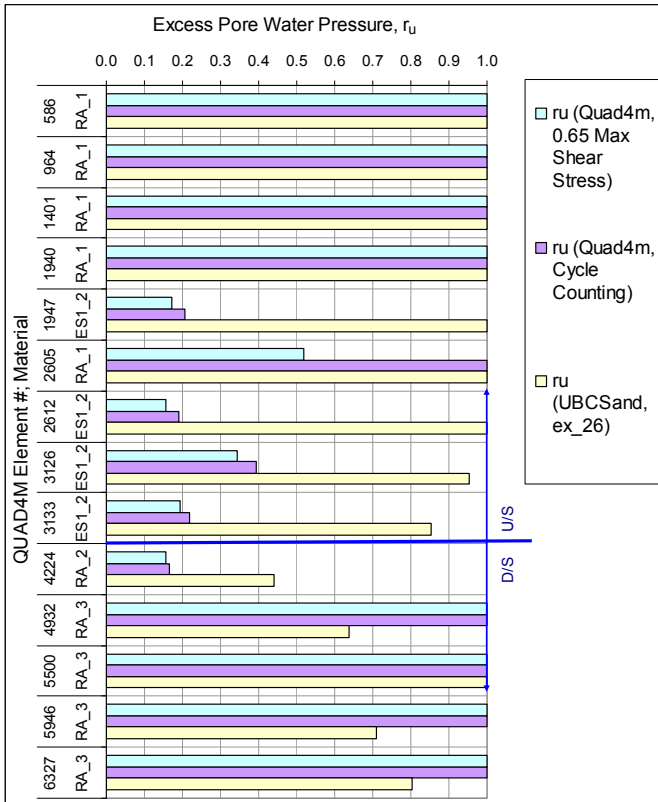


Figure 17. Comparison of Estimated r_u for MCE 14.

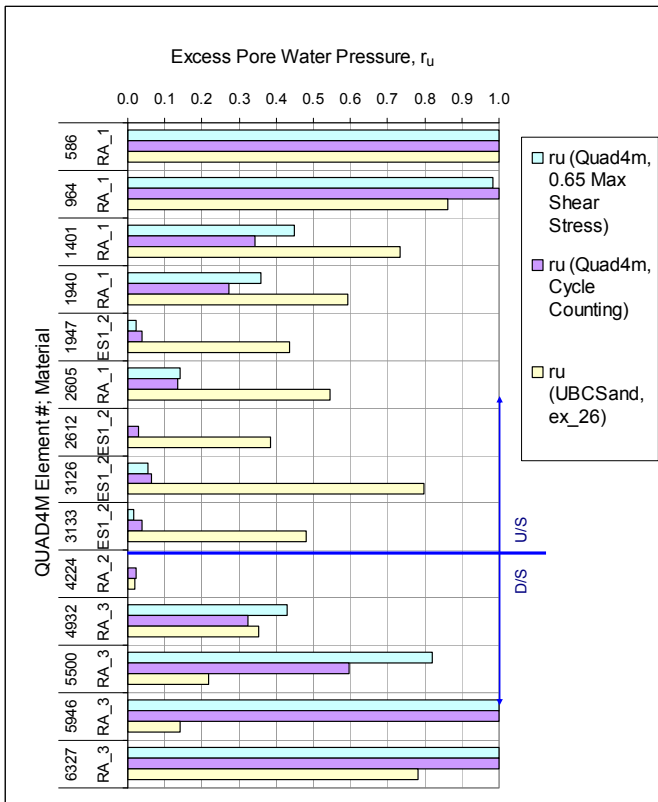


Figure 18. Comparison of Estimated r_u for OBE #8.

Supplemental analyses demonstrated that similar extents of predicted liquefaction of the foundation materials resulted in very similar failure slope geometries; however, the extent of liquefaction estimated by FLAC-UBCSAND in the denser embankment shell materials appeared to have an impact on the calculated deformation of the embankment.

A closer comparison of the estimated excess pore water pressure ratio (r_u) between the three methods is shown in Figures 17 and 18. The comparisons include r_u estimated using UBSCAND and QUAD4M results using both the simplified liquefaction procedure and the cycle counting method. The comparison for MCE 14, shown in Figure 17, in general demonstrates prediction of more liquefied zones with the use of UBSCAND, especially in the denser zones. The comparison for OBE #8 is shown in Figure 18; and in general also demonstrates prediction of higher values of r_u with the use of UBSCAND, especially in the denser zones.

The denser zones with higher predicted values of r_u using UBSCAND were generally located directly above the lower density foundation materials. Therefore, predicted liquefaction of these zones was probably attributed to the redistribution of the pore pressure in excess during shaking, which is allowed in FLAC analysis but generally disregarded in simplified analyses. The inability to account for pore pressure migration in the simplified model is one of the limitations of the method, which could have an effect on the analysis.

The other limitation in using QUAD4M and simplified method to estimate values of liquefaction potential and r_u is in applying the equivalent linear analysis to model a non-linear soil behavior. Therefore, the analyses appear to have reduced reliability for higher ground motions and lower density or softer foundation soils where larger cyclic shear strains are predicted. Figure 19 below is a summary of the predicted cyclic shear stains from QUAD4M for MCE #14 and OBE #8.

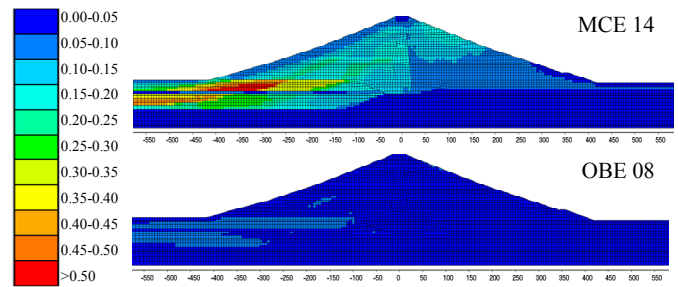


Figure 19. Comparison of Estimated Peak Cyclic Shear Strain (%) for MCE 14 and OBE #8.

As shown in Figure 19 the loading from MCE #14 was strong enough to induce peak cyclic shear strains in excess of 0.5% in most of the upstream foundation layers. This induced cyclic shear strain in lower foundation layers decreased the

stiffness of the materials and added damping to the materials, which influenced the response of the upper layers. For the upstream foundation materials (under MCE #14) the shear modulus was degraded on average by nearly 80%, while the average damping of the material was increased to nearly 20% (based on Figures 7 and 8). The decrease in the shear modulus and the increase in damping likely reduced the amount of energy that was transmitted to the embankment materials above, which may also explain the differences in the prediction of r_u between the QUAD4M-simplified method approach and UBCSAND.

CONCLUSIONS

Verification of FLAC results, in terms of acceleration amplification, induced cyclic stress and excess pore pressure can be successfully accomplished using the program QUAD4M coupled with the simplified procedure for liquefaction. However, in some cases the extent of predicted liquefied zones can be underestimated using the QUAD4M and coupled with the simplified liquefaction procedure approach due to the nature of the equivalent linear approach and the inability to account for pore pressure migration. In these cases, the UBCSAND model appears to better estimate excess pore water pressure generation and liquefaction potential.

REFERENCES

Andrus, R.D., and Stokoe, K.H., II [2000], "Liquefaction of Soils from Shear-Wave Velocity", *J. Geotech. and Geoenviron. Engrg.*, Vol. 126(11), 1015-1025.

Boulanger, R. W. [2003a]. "Relating K_α to Relative State Parameter Index", *J. Geotech. and Geoenviron. Engrg.*, Vol. 129(8), 770-773.

Boulanger, R. W. [2003b]. "High Overburden Stress Effects in Liquefaction Analyses." *J. Geotech. and Geoenviron. Engrg.*, Vol. 129(12), 1071-1082.

Boulanger, R. W. and Idriss, I. M. [2004a]. "State normalization of penetration resistances and the effect of overburden stress on liquefaction resistance." *Proc., 11th International Conference on Soil Dynamics and Earthquake Engineering, and 3rd International Conference on Earthquake Geotechnical Engineering*, D. Doolin et al., eds., Stallion Press, Vol. 2, 484-491.

Boulanger, R. W., and Idriss, I. M. [2004b]. Evaluating the potential for liquefaction or cyclic failure of silts and clays. Report UCD/CGM-04/01, Center for Geotechnical Modeling, University of California, Davis, CA, 130 pp.

Byrne, P.M., Park, S.S., Beaty, M., Sharp, M.K., Gonzalez, L., and Abdoun, T. [2004]. "Numerical modeling of liquefaction and comparison with centrifuge tests," *Canadian Geotechnical Journal*, Vol. 41(2):193-211.

Green RA, Terri GA [2005]. "Number of Equivalent Cycles Concept for Liquefaction Evaluation-Rrevisited. *J. Geotech. and Geoenviron. Engrg.*, Vol. 131(4):477-488.

Idriss, I. M., and Boulanger, R. W. [2007]. "Residual shear strength of liquefied soils." *Proceedings, Modernization and Optimization of Existing Dams and Reservoirs, 27th Annual United States Society on Dams Conference, USSD, Philadelphia, PA, 621-634.*

Itasca Consulting Group [2008]. "FLAC, Fast Lagrangian Analysis of Continua, Version 6.0", Itasca Consulting Group, Minneapolis, Minnesota, USA.

Marcuson, W. F. III, Hynes, M. E., and Franklin, A. G. [1990]. "Evaluation and Use of Residual Strength in Seismic Safety Analysis of Embankments," *Earthquake Spectra*, Vol. 6, No. 3, 529-572.

Ruthford, M., Perlea, V., and Beaty, M. [2008], "Deformation Analyses for Seismic Rehabilitation of Success Dam" *Dam Safety 2008, ASDSO, September 7-11, 2008, Indian Wells, California (proceedings available on CD).*

Schnabel, P. B. [1973]. *Effects of Local Geology and Distance from Source on Earthquake Ground Motions*. Berkeley, University of California. Ph.D. Thesis.

Seed, R.B. and Harder, L.F. [1990]. "SPT-based analysis of cyclic pore pressure generation and undrained residual strength." in J.M Duncan ed., *Proc., H. Bolton Seed Memorial Symposium, University of California, Berkeley*, Vol. 2, 351-376.

Seed, H.B. and Idriss, I.M. [1970]. "Soil moduli and damping factors for dynamic response analysis," Rpt. No. UCB/EERC-70/10, U.C. Berkeley, December.

Sun, J. I. G., R. & Seed, H.B. [1988]. *Dynamic Moduli and Damping Ratios for Cohesive Soils*. Berkeley, University of California.

Youd, T. L. et al. [2001] "Liquefaction Resistance of Soils: Summary Report from the 1996 NCEER and 1998 NCEER/NSF Workshops on Evaluation of Liquefaction Resistance of Soils", *J. Geotech. and Geoenviron. Engrg.*, Vol. 127(10), 817-833.